

Suppression of Transient Vibration for Geared Mechanical System Using Model-Based Control

Masahiko Itoh

1. Introduction

In geared mechanical systems such as industrial machines and industrial robots, several kind of machine elements including gear reducers are used between output shafts of motors and driven machine parts. The insufficiency of the torsional stiffness of these mechanical elements often induces transient vibrations mainly related to the eigenvalues in the lower-frequency range when the motor starts or stops. This transient vibration causes a problem such that the tact time of the system can not be shortened.

To solve this problem, the full-closed loop control which feeds back the state variables measured with sensors at the end effector.⁽¹⁾, the state-feedback control using observers⁽²⁾⁽³⁾, the load velocity feedback control with a disturbance observer⁽⁴⁾ and the dynamic damper comprised of the software⁽⁵⁾ have been proposed. However, the full-closed loop control technique and the control technique using an additional sensor are hard to set up in reality and incur increasing the cost. Further, the conventional observer technique to suppress the transient vibration requires a precise model of the mechanical system and an additional low-pass filter in a compensating loop. As a result, the observer technique has difficulties in setting up and adjusting its parameters in the field.

This paper deals with "a model-based control" for eliminating the transient vibration of a geared mechanical system. The control model is related to the velocity control loop though the conventional observer method is constructed in the torque control loop as a local feedback loop, and is composed of reduced-order electrical and mechanical parts by considering that the transient vibration which should be eliminated is mainly dominated by the first vibration mode in the geared mechanical system. The purpose of this method is to simplify the construction of the control system and the adjustments of its parameters.

This report describes how transient vibration is effectively reduced by applying this method to the torsional vibration system equipped with a harmonic drive gear reducer.⁽⁷⁾

2. Reduced-Order Model of Geared Mechanical System

2.1 Equation of Motion

As a typical example of an actual machine system equipped with a reduction gear mechanism, the rotary drum drive system shown in [Fig. 1](#) is taken up. This is a commonly-used machine system, which consists of 3 masses such as a motor rotor, a reducer's output shaft and a drum. Further, this machine system is often controlled by the PI type velocity control loop.

Equations of motion of 3 mass system are written as:

$$\left. \begin{aligned} J_m \ddot{\theta}_m + (C_g/R_g) (\dot{\theta}_m/R_g - \dot{\theta}_g) + (K_g/R_g) (\theta_m/R_g - \theta_g) &= T_m \\ J_g \ddot{\theta}_g + C_g (\dot{\theta}_g - \dot{\theta}_m/R_g) + K_g (\theta_g - \theta_m/R_g) \\ &+ (C_l/R_l) (\dot{\theta}_g/R_l - \dot{\theta}_l) + (K_l/R_l) (\theta_g/R_l - \theta_l) = 0 \\ J_l \ddot{\theta}_l + C_l (\dot{\theta}_l - \dot{\theta}_g/R_l) + K_l (\theta_l - \theta_g/R_l) &= 0 \end{aligned} \right\} \dots (1)$$

θ_m : angular rotation of the motor

θ_g : angular rotation of the gear reducer's output shaft

θ_l : angular rotation of the driven machine

T_m : output torque of the motor

J_m : moment of inertia of the motor

J_g : moment of inertia of the reducer's output shaft

J_l : moment of inertia of the driven machine (drum)

R_g : reduction ratio of the gear reducer

K_g : torsional stiffness of the reducer

C_g : damping factor of the reducer

R_l : reduction ratio between the reducer's output shaft and the driven machine

K_s : torsional stiffness between the reducer's output shaft and the driven machine

C_s : damping factor between the reducer's output shaft and the driven machine

The voltage of the armature circuit can be expressed by the Eq. (2), taking the counter-electromotive voltage and the inductance of the armature winding into consideration in the servo motor that is velocity-controlled by the PI control.

$$\left. \begin{aligned} L \frac{di}{dt} &= K_t (K_e e + \frac{K_v}{T_i} \int e dt - K_{ai} i) - Ri - K_e \omega_m \\ e &= \omega_{cmd} - \omega_m \end{aligned} \right\} \dots (2)$$

The output torque of the servo motor is given by:

$$T_m = K_t i \dots (3)$$

where

ω_{cmd} : velocity command

ω_m : rotating speed of the motor (= rotating speed of the wave generator)

ω_g : rotating speed of the gear reducer's output shaft

ω_l : rotating speed of the driven machine

e : error

i : current of the armature

R : motor armature resistance

L : motor armature inductance

K_t : torque constant

K_e : voltage constant

K_c : current loop gain

K_{cb} : current feedback gain

K_v : proportional gain of the PI control

K_{cb} : integral time constant of the PI control

According to Eqs. (1)~(3), a block diagram of the geared mechanical system can be expressed as [Fig. 2](#).

2.2 Reduced-Order Model of Mechanical Part

Most of geared mechanical systems can be grouped into two classes due to the insufficiency of the torsional stiffness. The first case is that the stiffness of a geared stage is much higher than those of a shaft, a coupling and a timing belt. The second case is that the stiffness of a geared stage is much lower than that of a driven part such that a rigid body is directly connected to the reducer's output shaft. This drum driving system can be regarded as the first case.

Consequently, this paper deals with a case such that the residual vibration is mainly dominated by the first vibration mode and the higher order vibration modes are apart from the first one. As a result, the 3 mass system shown in Fig. 2 is transformed into a 2 mass system shown in Fig. 3 by considering only the first vibration mode. In this reduced-order model, the natural angular frequency ω_n and the damping ratio γ_n are expressed as

$$\left. \begin{aligned} \omega_n &= \sqrt{K_r^m (1/J_m^m + 1/J_l^m)} \\ \gamma_n &= \frac{C_r^m (1/J_m^m + 1/J_l^m)}{2\omega_n} \end{aligned} \right\} \dots (4)$$

where

$$\left. \begin{aligned} J_m^m &= J_m + J_l / R_g^2 \\ J_l^m &= J_l / (R_g^2 R_r^2) \\ K_r^m &= K_r / (R_g^2 R_r^2) \\ C_r^m &= C_r / (R_g^2 R_r^2) \end{aligned} \right\} \dots (5)$$

Here, the superscript "m" shows that parameters belong to the model. Defining the inertia ratio $R_n \equiv J_l^m / J_m^m$ and transforming Eq. (4), J_l^m , K_r^m and C_r^m are expressed as

$$\left. \begin{aligned} J_l^m &= R_n J_m^m \\ K_r^m &= \frac{R_n J_m^m}{1+R_n} \omega_n^2 \\ C_r^m &= \frac{2R_n J_m^m}{1+R_n} \gamma_n \omega_n \end{aligned} \right\} \dots (6)$$

Using these expression, the reduced order model can be easily obtained from not only design data but also measured data of ω_n and γ_n in the actual system.

2.3 Reduced-Order Model of Electrical Part

The reduced-order model of the electrical part is created on the block diagram shown in Fig. 2. Here, the effect of the counter electromotive force is ignored. Further, considering that the angular cut-off frequency ω_c of the current control loop is much higher than the first natural angular frequency of the mechanical system and the current loop gain within ω_c is about 1.0, the current control system composed of the current loop and the torque constant is expressed as a proportional gain K_t^m . As a result, a simplified PI control system is obtained as shown in Fig. 3. Expressing the natural angular frequency ω_e and the damping ratio ξ_e of the electrical part as Eq. (7), the parameters of reduced-order model can be easily adjusted.

$$\left. \begin{aligned} \omega_r &= \sqrt{\frac{K_r^m K_r^m}{T_i^m J_m^m}} \\ \zeta_r &= \frac{1}{2} \sqrt{\frac{T_i^m K_r^m K_r^m}{J_m^m}} \end{aligned} \right\} \dots (7)$$

where $K_v^m = K_v$ and $T_i^m = T_i$.

3. Model-Based Control

3.1 Control System

The block diagram of the reduced-order model shown in Fig. 3 is equivalently converted to the dotted area in Fig. 4, using equations (4) to (7). Fig. 4 shows a block diagram of the model-based control system using the control model for the velocity control system. The purpose of the model-based control is to suppress the residual vibration dominated by the first vibration mode of the mechanical system. Here, the value of R_t is set to 1.0 as a general case.

In the compensating control system, the difference between the load's speed ω_l^m which is estimated at the motor shaft and the motor speed ω^m is dynamically calculated, and it is multiplied by gain K_b . Finally, $K_b (\omega_l^m - \omega^m)$ is added to velocity command ω_{cmd} as follows:

$$\omega'_{cmd} = \omega_{cmd} + K_b (\omega_l^m - \omega^m) \dots (8)$$

In other words, in this configuration the amount of feedforward compensation $K_b (\omega_l^m - \omega^m)$ is added to the velocity command ω_{cmd} , which is converted to the velocity command ω'_{cmd} in the actual system.

3.2 Simulation of Frequency Response

The parameter values of the actual system and the model system that are used for simulation are shown in Table 1. The frequency response of the transfer function ω_l / ω_{cmd} is shown in Fig. 5. Gain K_b is set to 0.75 for these simulations. Fig. 5 shows that the model-based control increases the damping coefficient between the load and the reducer's output shaft equivalently.

3.3 Simulation of Step Response

Next, the step response is calculated using the Runge-Kutta method to verify the effect of suppressing transient vibration when the model-based control is used. Fig. 6 shows the simulation results. In this simulation, the velocity command is changed from 0 to 1000 min^{-1} , then from 1000 to 0 min^{-1} as a step response. Gain K_b is set to 0.75 in this case, too. It is clear that the damping ratio of the mechanical system is increased and the settling time of the transient vibration of the load can be reduced down to about 1/3.3 (from 200 to 60ms).

4. Experimental Results and Considerations

4.1 Experimental Set-Up

An outline of the experimental set-up is shown in Fig. 7. A harmonic drive reducer with a reduction ratio of 1/50 is attached to the motor. A load is attached to its output shaft via a torsion-bar. This experimental set-up shows a case study of $R_t=1$ concerning a 3 mass system shown in Fig.2. Physical parameters of the experimental

set-up are shown in [Table 2](#). The first natural frequency of the mechanical system is 31Hz and the damping ratio is 0.08.

4.2 Construction of Control System

The velocity control system of the main loop consists of a software servo. The velocity command is generated from a personal computer. The sampling time of this loop is 0.4 ms.

On the other hand, the compensation loop composed of the reduced-order model is integrated into a DSP (TMS320C25 of Texas Instruments) after the digital re-design using a backward difference method (6) based on the simulation result. The sampling time of this compensation loop is 1.2 ms. Gain K_b is set to 0.75 according to the simulation result.

4.3 Effects on Residual Vibration

[Fig. 8](#) shows the suppression effect on the residual vibration when the motor starts. In this experiment, the motor velocity command is changed from 0 to 1000 min^{-1} as a step input. The motor speed and the load speed are measured with an oscilloscope

[Fig. 8](#) shows that the model-based control suppresses the overshoot level of ωl down to about 1/1.5 and the settling time can be shortened down to about 1/3 (from 330 to 120msec). Here, the velocity ripple which occurs after the residual vibration is generated by the harmonic drive gear's excitation of 2 cycles/rev.

Next, [Fig. 9](#) shows the suppression effect on the residual vibration when the motor stops suddenly. The motor velocity command is changed from 1000 to 0 min^{-1} as a step input. [Fig. 9](#) shows that the proposed model-based control suppresses the overshoot level of ωl down to about 1/1.5 and the settling time can be shortened down to about 1/3 (from 270 to 90msec).

5. Conclusions

A model-based control is described as a technique of eliminating the residual vibration generated at a final stage of loading. This control model is composed of electrical and mechanical parts of the velocity control loop. This control model obtained from design data or experimental data is easily integrated into a DSP.

This control technique is applied to a mechanical system which is equipped with a harmonic drive gear reducer whose reduction ratio is 1/50 and a load connected to the reducer's output shaft through a torsion-bar. Simulations and experiments on the step responses show satisfactory control results in reducing the transient vibration of the loading inertia. As a result, the setting time can be shortened down to about 1/3 of the uncompensated level and the overshoot of the transient vibration can be suppressed down to about 1/1.5.

References

- (1)Futami, S. et al.: "Vibration Absorption Control of Industrial Robots by Acceleration Feedback," *IEEE Trans. Ind. Elect.*, 30-3 (1983), pp. 299 - 305.
- (2)Yuki, K. et al.: "Vibration Control of a 2 Mass Resonant System by the Resonance Ratio Control," *Trans. IEE Japan*, (in Japanese), 113(D)-10(1993), pp.1162 - 1169.
- (3)Honke, K. et al.: "Motion and Vibration Control for Robot Arm with Elastic Joint (Application of Disturbance Observer Including Elastic Vibration)," *Trans. Jpn. Soc. Mech. Eng.* (in Japanese), 60-577(1994), pp. 3045 - 3050.

- (4)Godler, I. et al.: "Vibration Suppression for a Speed Control System with Gear," J. Jpn. Soc. Prec. Eng., (in Japanese), 60-1(1994), pp. 86 - 90.
- (5)Sakuta, H. et at.: "Vibration Absorption Control of Robot Arm by Software Servomechanism (2nd Report)," Trans. Jpn. Soc. Mech. Eng., (in Japanese), 54-497(1988), pp. 217 - 220.
- (6)For example, Mita, T., "Introduction to Digital Control," (in Japanese), (1989), 115 - 118, Corona Publishing.
- (7)Itoh, M. and Kase, S.: "Suppression of Transient Vibration for Geared Mechanical System (Effects of Model-Based Control)," Trans. Jpn. Soc. Mech. Eng., (in Japanese), 64 - 623(1998), pp. 2596 - 2601.
-

Masahiko Itoh

Joined company in 1988

Technology Development Division

Worked on study and development of motion and vibration control

Doctor of Engineering

Table 1 Simulation conditions

Parameter		Value	Unit
1. Moment of inertia	J_m	1.765×10^{-5}	$\text{kg} \cdot \text{m}^2$
	J_g	7.548×10^{-6}	
	J_l	3.422×10^{-4}	
2. Torsional stiffness	K_g	5053.5	$\text{N} \cdot \text{m}/\text{rad}$
	K_s	12.769	
3. Damping coefficient	C_g	0.13	$\text{N} \cdot \text{m} \cdot \text{s}/\text{rad}$
	C_s	0.0108	
4. Gear reducer			
Reduction ratio	R_g	50.0	
5. Velocity loop gain	K_v	0.01	$\text{A}/(\text{rad}/\text{s})$
6. Integral time constant	T_i	0.02	sec
7. Torque constant	K_t	0.316	$\text{N} \cdot \text{m}/\text{A}$
8. Voltage constant	K_e	0.316	$\text{V}/(\text{rad}/\text{s})$
9. Phase resistance	R	4.5	Ω
10. Phase inductance	L	0.0189	H
11. Current loop gain	K_c	118.84	V/A
12. Current feedback gain	K_{cb}	1.0	
13. Feedback gain	K_b	0.75	
14. Reduced-Order Model			
Moment of inertia	J_m^m	1.765×10^{-5}	$\text{kg} \cdot \text{m}^2$
	J_l^m	1.369×10^{-7}	
Torsional stiffness	K_s^m	5.108×10^{-3}	$\text{N} \cdot \text{m}/\text{rad}$
Damping coefficient	C_s^m	4.32×10^{-6}	$\text{N} \cdot \text{m} \cdot \text{s}/\text{rad}$
Velocity loop gain	K_v^m	0.01	$\text{A}/(\text{rad}/\text{s})$
Integral time constant	T_i^m	0.02	sec
Torque constant	K_t^m	0.316	$\text{N} \cdot \text{m}/\text{A}$

Table 2 Physical parameters of the experimental set-up

Parameter		Value	Unit
Moment of inertia	J_m	1.765×10^{-5}	$\text{kg} \cdot \text{m}^2$
	J_g	7.548×10^{-6}	
	J_l	3.422×10^{-4}	
Torsional stiffness	K_g	5053.5	$\text{N} \cdot \text{m}/\text{rad}$
	K_s	12.769	
Damping coefficient	C_g	0.13	$\text{N} \cdot \text{m} \cdot \text{s}/\text{rad}$
	C_s	0.0108	
Reduction ratio of gear reducer	R_g	50.0	

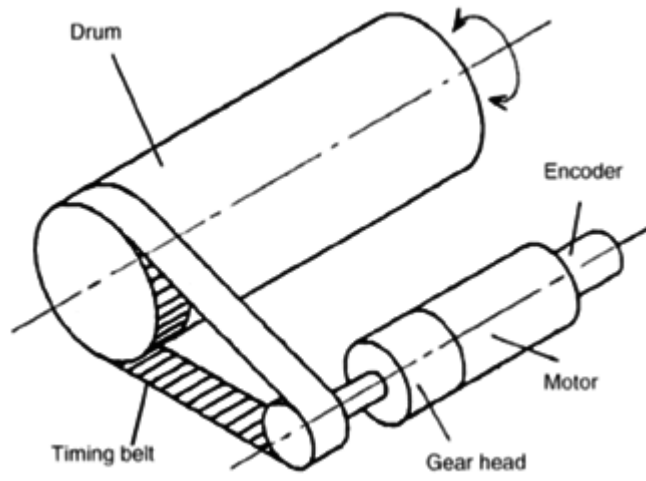


Fig. 1 Example of geared mechanical system

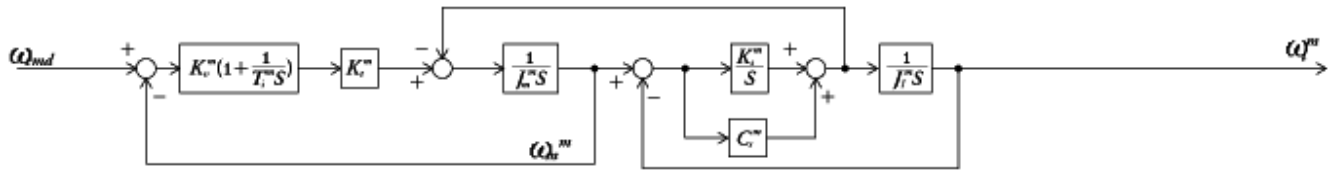


Fig. 3 Block diagram of reduced-order system

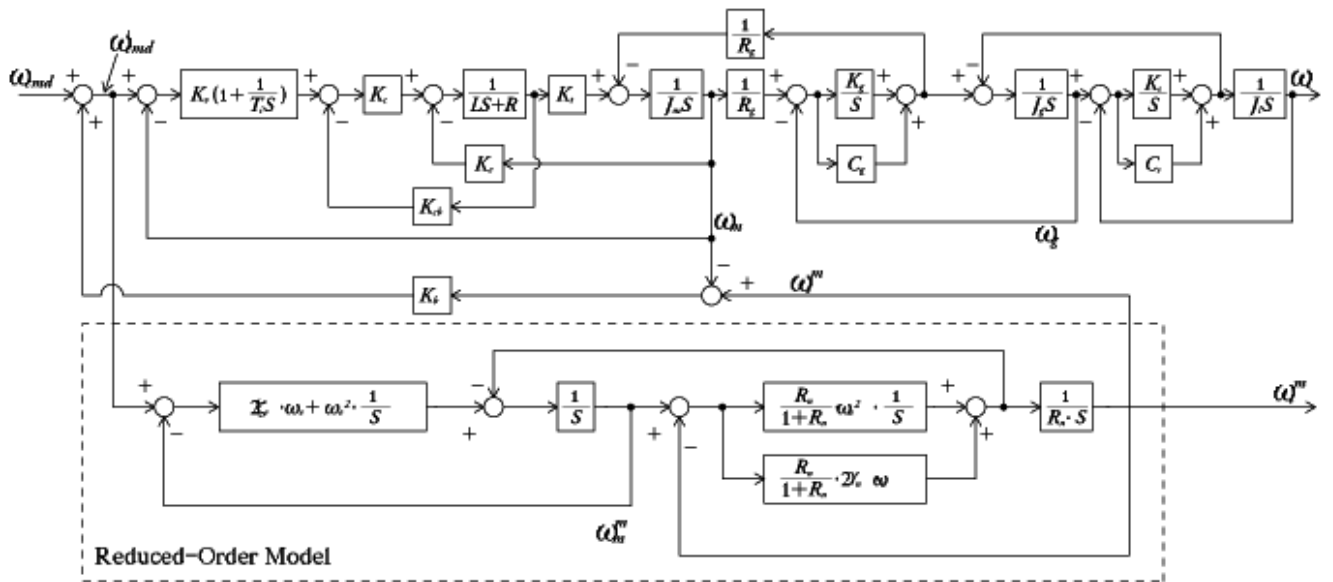
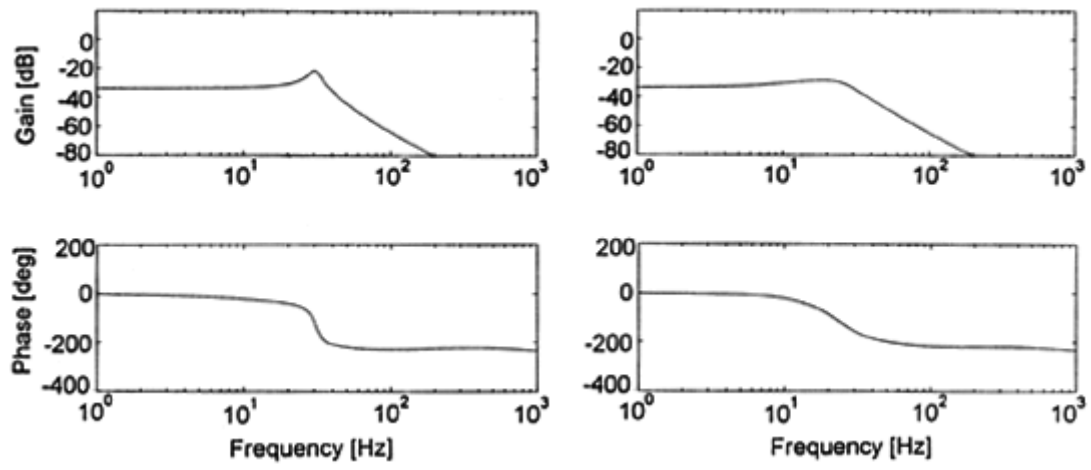


Fig. 4 Block diagram of model-based control



(a) Without model-based control

(b) With model-based control

Fig. 5 Simulation results of ω_l / ω_{cmd}

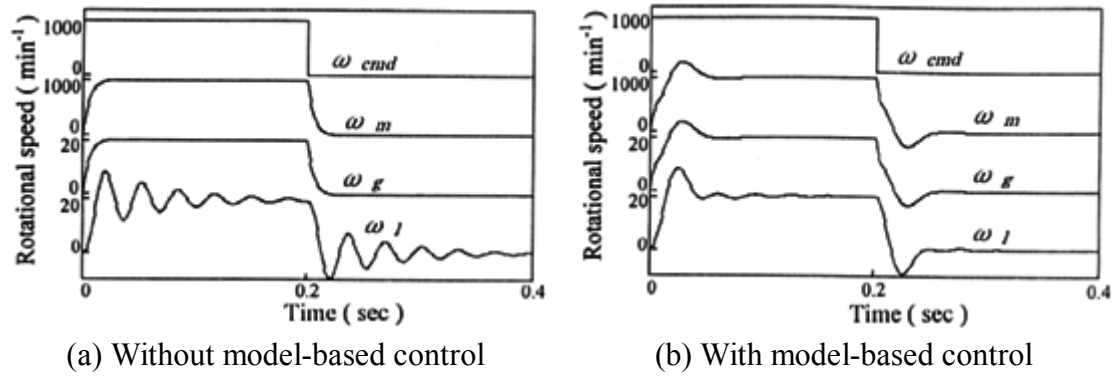


Fig. 6 Simulation results of step response

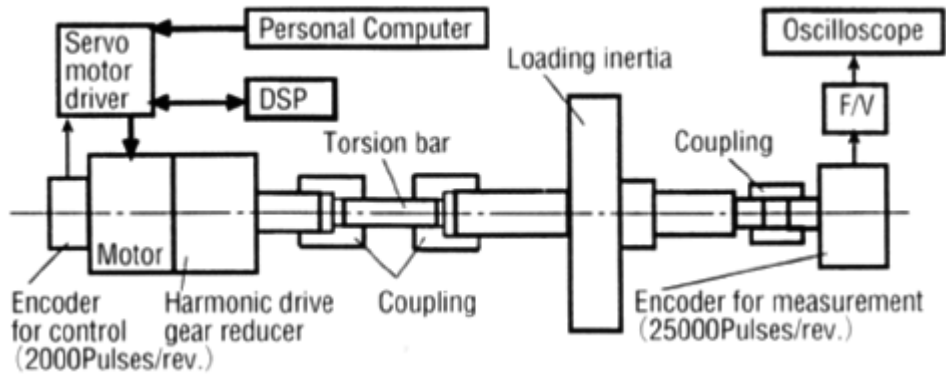
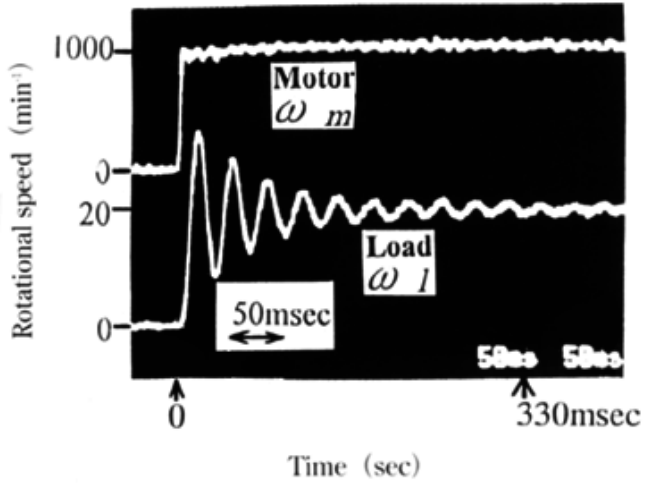
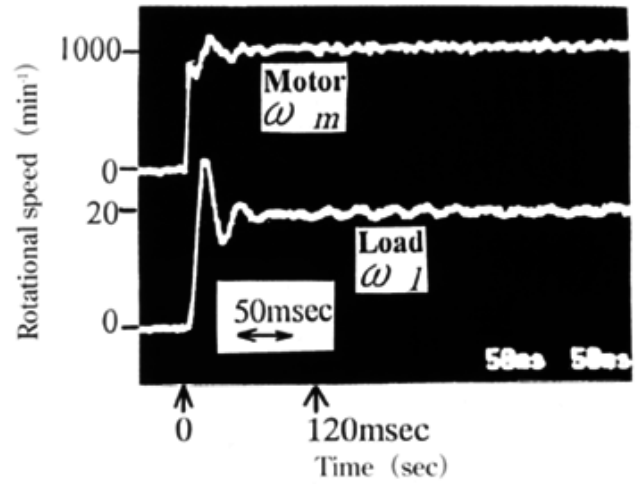


Fig. 7 Schematic diagram of the experimental set-up

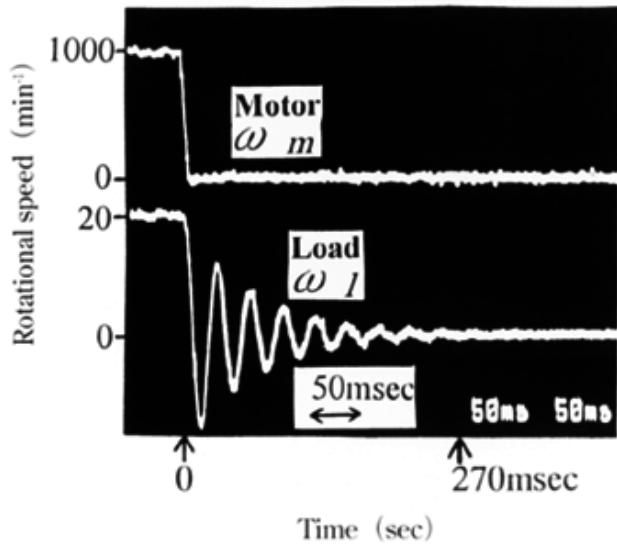


(a) Without model-based control

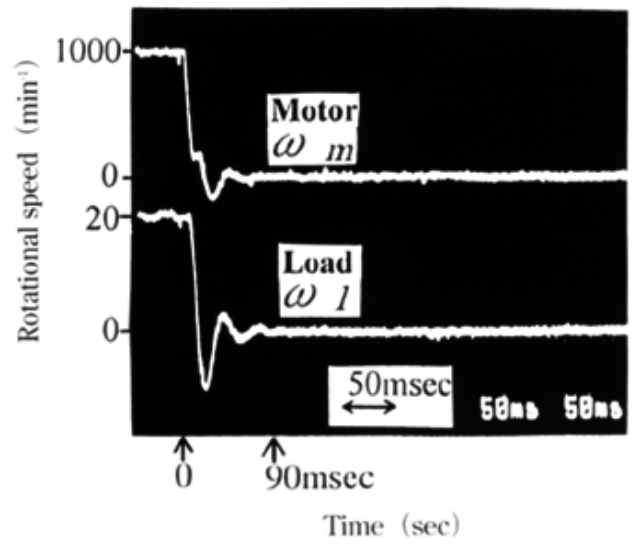


(b) With model-based control

Fig. 8 Experimental results of step response (at starting)



(a) Without model-based control



(b) With model-based control

Fig. 9 Experimental results of step response (at stopping)